Mechanical properties of non-reconstructed defective single-wall carbon nanotubes

2009 J. Phys. D: Appl. Phys. 42 142002

(http://iopscience.iop.org/0022-3727/42/14/142002)

IOP PUBLISHING
IOP FTC
JOURNAL OF PHYSICS D: APPLIED PHYSICS
J. Phys. D: Appl. Phys. **42** (2009) 142002 (6pp)
doi:10.1088/0022-3727/42/14/142002

FAST TRACK COMMUNICATION

Mechanical properties of non-reconstructed defective single-wall carbon nanotubes

F Scarpa[1,3], S Adhikari[2] and C Y Wang[2]

[1] Advanced Composites Centre for Innovation and Science, University of Bristol, BS8 1TR Bristol, UK
[2] School of Engineering, Swansea University, Swansea, UK

E-mail: f.scarpa@bris.ac.uk and scarpa.fabrizio@gmail.com

Received 8 April 2009, in final form 25 May 2009
Published 26 June 2009
Online at stacks.iop.org/JPhysD/42/142002

Abstract
This paper describes the equivalent homogeneous uniaxial mechanical properties of defective single-wall carbon nanotubes. In particular, non-reconstructed defects that can be produced by ion or electronic irradiation have been considered. A discrete nonlinear finite-element approach based on the mechanical properties of individual carbon–carbon (C–C) bonds has been used. The individual C–C bonds in turn were simulated as beam structural elements. Extensive Monte Carlo based numerical simulation has been reported in the paper. The results show that the homogeneous elastic properties of the defective nanotubes can be qualitatively and quantitatively different from the pristine configurations. The defective nanotubes show a slight reduction in axial stiffness (Young's modulus), but large variations of Poisson's ratio outside the elastic bounds for isotropic materials, depending on the locations of the vacancies. The large fluctuations of Poisson's ratio can lead to extreme positive transversal contractions or to auxetic behaviour when the nanotubes are subjected to tensile loading.

(Some figures in this article are in colour only in the electronic version)

Poisson's ratio (PR) indicates the level of transversal contraction of a material or structure when loaded along one direction. In isotropic, homogeneous and thermodynamically stable materials, the PR varies between -1 and 0.5, where the higher bound corresponds to an incompressible (rubber-like) solid, while the negative limit is related to a solid with infinite shear modulus. In anisotropic materials, Poisson's ratios can vary beyond the above bounds, the reciprocity relation between PRs and Young's moduli being the only thermodynamic constraint for special orthotropic materials, for example [1]. The negative Poisson's ratio (NPR) is also a peculiar characteristic, leading to a counter-intuitive deformation mechanism where a tensile loading provides a transverse expansion of the material. NPR, or auxetic behaviour, has been observed experimentally in iron pyrite [2] at the beginning of the twentieth century, and subsequently confirmed for 69% of the cubic elemental metals and some face-centred cubic (fcc) rare gas solids, when stretched along the specific [1 1 0] off-axis direction [3]. Artificially made materials and structures exhibiting NPR behaviour have been manufactured as open cell foams [4], long fibre composites [5], microporous polymers [6] and honeycomb structures [7, 8]. The rationale behind the interest in unusual NPR solids stems from their increased hardness and bending resistance [9], and the experimental evidence that auxetic honeycombs and foams provide enhanced flatwise compression [10] and indentation [11], acoustic absorption [12] and dielectric loss [13] compared with their positive Poisson's ratio counterparts.

According to various nanomechanical models [14, 15], Poisson's ratio of single-wall carbon nanotubes (SWCNTs) vary between 0.29 and 0.16, along with the chirality of the nanostructure. At the nanoscale level, the possibility of having

[3] Author to whom any correspondence should be addressed.

carbon nanotube (CNT) structures with NPR behaviour has been reported by Jindal and Jindal [16] and Yao *et al* [17], when weakening of the C–C bond strength and variation of its length could be considered. *Ab initio* simulations from Van Lier *et al* have shown that marginally NPR behaviour (−0.032) could be achieved in closed short (9,0) SWCNTs [18]. Yakobson and Couchman [19] have also pointed out that NPR could be achieved in CNT bundles when an extension of an entangled mat in one direction releases a relative glide of the CNTs filaments at their crossing. Evidence of this type of in-plane NPR behaviour has recently been discovered in buckypapers, with mixed MWCNTs–SWCNTs arrays, with PR values up to −0.3 for nanotubes average orientations of 50° in the CNT sheet [20].

In this paper, we have discovered evidence of extreme positive and NPR (auxetic) behaviour in defective SWCNTs. These defects are due to the presence of non-reconstructed vacancies (NRVs) [21]. CNTs, originally thought to be almost defect free, could have a high density of defects that are introduced by (a) particular synthesis techniques, e.g. chemical synthesis [22], or created deliberately by (b) the chemical treatment in the purification process [23, 24] and (c) irradiation to achieve desired functionality [25–27]. Specifically, vacancies [28, 29] and the Stone–Wales (SW) defects [29–34] are most frequently found in CNTs. In the defects of vacancy, there are only two axial orientations mutually distinguishable at $2\pi/3$. Although metastable, the non-reconstructed SWCNT configurations can be present at low temperatures and low dose irradiation [36], as well as in configurations with dangling bonds surrounded by a polymer matrix or in MWCNTs and bundles of SWCNTs [37]. A lattice configuration similar to the one of NRVs has been hinted as a lattice topology to generate auxetic and extreme Poisson's ratio in open cell foams [39] and centresymmetric honeycombs [40].

To verify whether an extreme Poisson's ratio behaviour could be present in non-reconstructed defective SWCNTs, we have used an equivalent atomistic–continuum structural model, where the C–C bonds are represented by 3D structural beams having flexural, bending and torsional stiffness [41, 42]. In structural mechanics of nanoassemblies, the thickness of the C–C bond is an important parameter in determining the equivalent stiffness of the nanostructure, and the large scatter of thickness (and Young's modulus) present in the open literature is referred to as 'Yakobson's paradox' [43]. In our models, the thickness of the C–C bonds of the SWCNTs has been determined using an equivalent atomistic–continuum model based on the equivalence between the harmonic potential expressed through the AMBER force model and structural shear beam strain energies [44, 45]. The thickness of the C–C bond identified using this method is 0.084 nm, with an equilibrium bond length of 0.142 nm, leading to Young's axial and flexural modulus for armchair and zigzag configurations in good agreement with MD-based simulations and experimental results in the open literature. SWCNT models were assembled using Finite Element 3D structural beams equivalent to C–C bonds for different armchair and zigzag configurations with chiral index $n = 6, 13, 20, 27$. The lengths of the CNTs were varying with aspect ratios (tube length/diameter) of 5, 10, 15 and 20. The vacancies were simulated selecting atoms using a random Latin Hypercube sampling technique, and deactivating the connected C–C bonds providing the 120° axial directions for the single defect. The defective CNTs were modelled using four different percentages of vacancies over the total number of atoms in a single CNT—0.5%, 1.0%, 1.5% and 2.0%, providing a structure with distributed NRVs like the one of figure 1. To simulate the uniaxial loading, the nanotubes were clamped at one end, and subjected to a uniaxial strain $\bar{\varepsilon}_z$ of 0.1% under a nonlinear geometric loading condition. The uniaxial strain was applied imposing a corresponding uniform displacement at the free end of the tube. Each atom's radial strain ε_r was calculated as the ratio between the radial deformation after loading and the SWCNT radius. The homogenized radial strain for the whole CNT was then calculated in integral form as $\bar{\varepsilon}_r = \int \varepsilon_r \mathrm{d}S/S$, where S is the surface of the tube. Young's modulus and Poisson's ratio ν_{rz} were estimated using the following definitions:

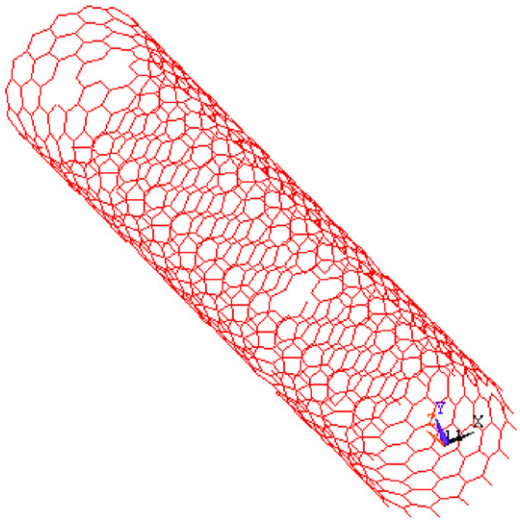

Figure 1. Zigzag (13, 0) nanotube with aspect ratio of 10 having 2.0% of NRVs.

$$Y = \frac{\sigma_z}{\bar{\varepsilon}_z}, \qquad \nu_{rz} = -\frac{\bar{\varepsilon}_r}{\bar{\varepsilon}_z}, \tag{1}$$

where the stress σ_z was calculated averaging the axial forces at the loaded end of the nanotube. For each nanotube configuration, 200 Monte Carlo sampling of vacancies were performed, providing a total of 25 600 simulations for zigzag and armchair tubes. The FE simulations were carried out using the commercial code ANSYS Multiphysics [46].

The presence of the non-reconstructed defects provides a general decrease in Young's modulus. As a general trend for all the chiralities considered, the decrease in average axial stiffness depends mildly on the radius and aspect ratio of the nanotubes, while the percentage of vacancies appears to be the most important factor (figure 3(*a*)). For example, in armchair tubes with aspect ratio 5, for a defects percentage of 0.5%, the mean value of the ratio between defected and pristine Young's modulus varies between 0.995 for a radius of 0.41 nm to 0.958 for a tube diameter of 3.2 nm, to slightly increase to 0.961 for a radius of 2.13 nm. This behaviour can also be observed for

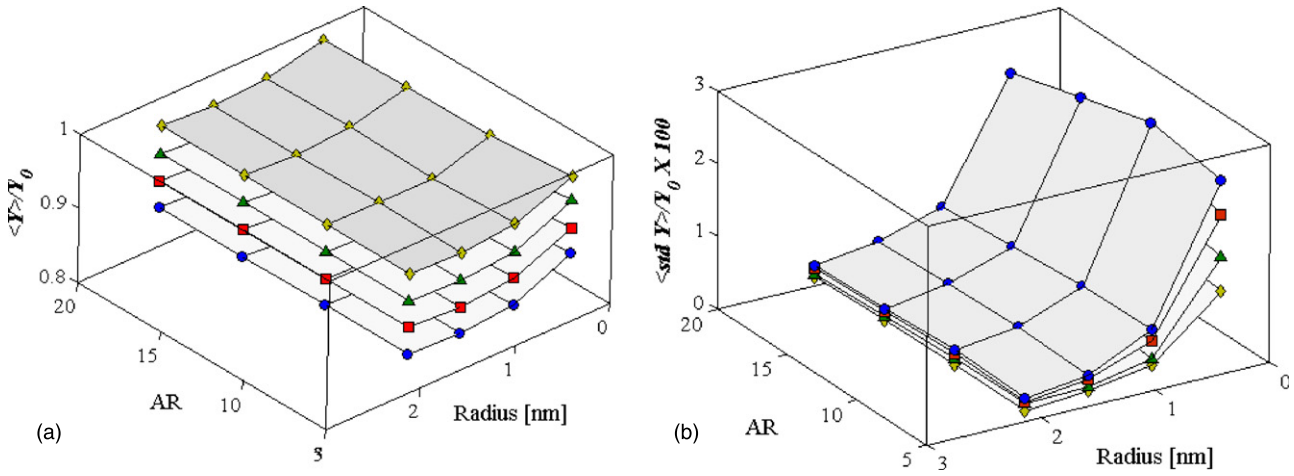

Figure 2. (*a*) Ratio between mean of axial Young's modulus and pristine stiffness and (*b*) between standard deviation of Young's modulus against pristine Young's modulus for armchair (n, n). Pristine Young's modulus Y_0: 2.9, 1.36, 0.91, 0.67 TPa for a thickness $d = 0.084$ nm. ● = 2% NRV; ■ = 1.5% NRV; ▲ = 1% NRV; ♦ = 0.5% NRV.

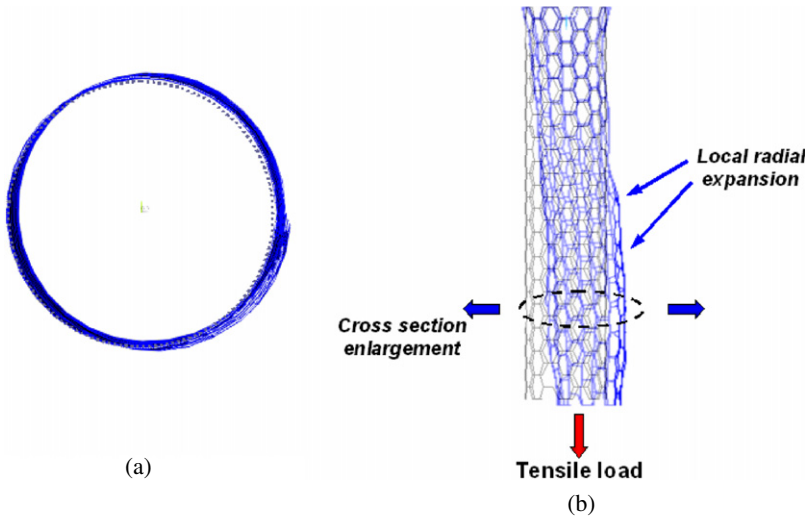

Figure 3. Zigzag (6, 0) with aspect ratio 10 and 2.0% of defects under axial tensile loading, with pristine Poisson's ratio $\nu_{rz} = 0.188$ and Young's modulus $Y_0 = 1.71$ TPa. (*a*) The cross section of the tube enlarges while the nanotube is pulled (undeformed configuration is the grey dottted line). The overall homogenized NPR coefficient (−0.932) is due to localized out-of-plane rotations caused by the NRVs, providing local enlargements along the radial direction (*b*).

increasing values of defects percentages, with a minimum of $\langle Y \rangle / Y_0$ of 0.85 for a tube with radius of 1.6 nm corresponding to 2% defects. Sammalkorpi *et al* [21] observe a Y/Y_0 ratio up to 0.97 in (5, 5) nanotubes with triple vacancies. A trend similar to the armchair tubes is also observed for the zigzag ones, with drops of the average axial stiffness versus the pristine one from 0.962 for 0.5% vacancies ratio to 0.825 for 2% of defects (radius = 0.88 nm for a tube aspect ratio of 15). The ratio between the standard deviation of Young's modulus versus Y_0 shows dependences versus the radius of the type R^{-1}, while the sensitivity versus the aspect ratio, AR, is remarkably low. We have noticed that the mean of the standard deviation versus the pristine Young's modulus is confined between a maximum of 2.7% for a radius of 0.43 nm, aspect ratio of 5 and NRV percentage of 2, to a minimum of 0.14% for radius of 2.14 nm, maximum aspect ratio of 20 and vacancies percentage of 0.5 (figure 2(*b*)). Analogous dependences versus the tubes radius, aspect ratios and NRV percentage were recorded for the zigzag configurations, both in terms of mean Young's modulus and its standard deviation distribution.

On the opposite, Poisson's ratio ν_{rz} in the defected nanotubes shows large variations, depending on the tube geometry, the percentage and the location of vacancies. We have observed that NPR is normally induced by defects close to the ends of the tube, and concurrently at the middle of the CNT length, as shown in figure 3 for a (6,0) nanotube. The NRVs close to the ends provide an amplification of the Saint-Venant effects [47] on the loading conditions (the distribution of the applied axial force and the clamping constraint at the opposite end), causing out-of-plane rotations of the C–C bonds connected to the vacancies, and local radial expansion of the nanotube under a positive axial strain. When the NRVs were located on average 4–5 cells away from the ends, the mechanical behaviour of the defected nanotubes was the opposite, with local radial contractions under a global positive axial strain, that is, when averaged over the tube length provide

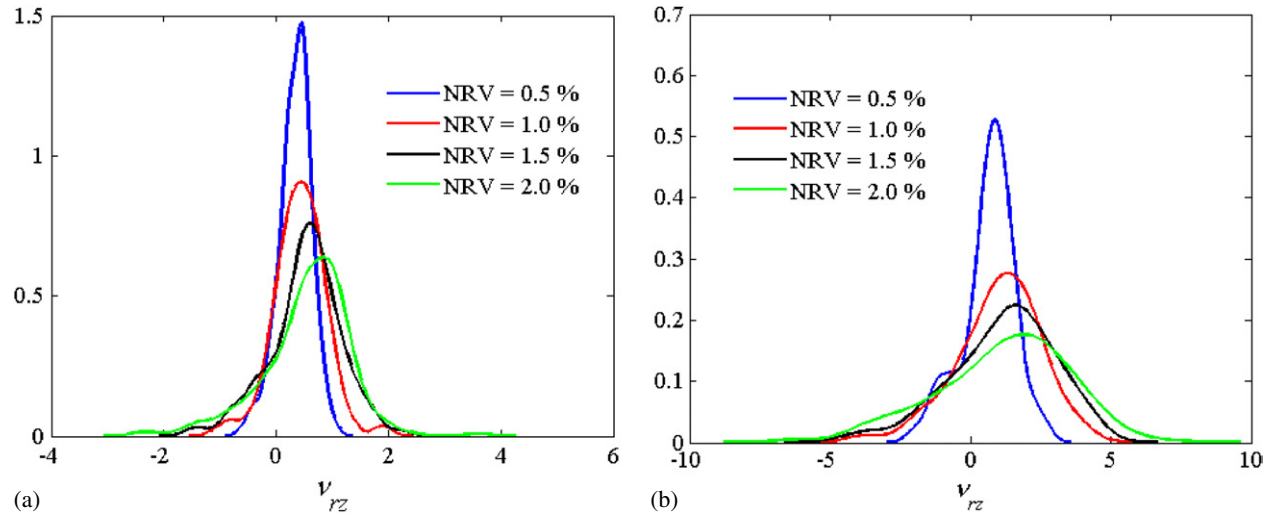

Figure 4. Probability density functions for Poisson's ratio in (*a*) armchair tubes ($R = 0.426$ nm, aspect ratio = 5, pristine $\nu_{rz} = 0.29$) (*b*) zigzag tubes ($R = 1.57$ nm, aspect ratio 20, pristine $\nu_{rz} = 0.167$).

a positive Poisson's ratio effect. Pristine single-wall nanotubes have Poisson's ratios ν_{rz} values varying with their chirality in the range 0.29–0.16 [14, 44, 48]. The non-reconstructed defective nanotubes showed significant variations in terms of magnitude and sign, for a given chirality, aspect ratio and percentage of NRVs. While the ratio between the standard deviation and mean value of Young's modulus were in the order of 0.1–2.7% according to the different vacancies percentages (figure 2(*b*)), the probability density functions associated with Poisson's ratio showed significant levels of skewness and, in general, a non-Gaussian distribution. For armchair tubes (6, 6) and aspect ratio of 5, the mean Poisson's ratio varies between 0.22 at a NRV percentage of 0.5 to 0.59 for NRV = 2% (figure 4(*a*)). Poisson's ratio ν_{rz} of the pristine nanotube is 0.29. The standard deviations are significantly large, ranging from 0.66 to 2.14–3 to 3.6 times the mean values. With the maximum aspect ratio considered in this study (20), the probability density distributions for Poisson's ratio show even higher average value and standard deviation discrepancies from the pristine nanotube values, as in the case of the zigzag nanotube (32,0) (figure 4(*b*)). The mean values range from 0.31 to 0.41, while the standard deviations fluctuate between 1.9 and 5.39, according to the NRV percentages. These values of Poisson's ratio make the NRD nanotubes anisotropic materials, such as tubular auxetic truss structures studied previously by some of the authors, albeit with larger ν_{rz} values available [49]. The 'missing rib' mechanism [39] has shown the possibility of obtaining auxetic behaviour from unit cells with 4-connectivities at $2\pi/3$ internal angles. For these topologies, Poisson's ratio is equal to ~ -4 and fairly constant up to true engineering strains of 20%. However, in [39] the whole lattice of the honeycomb has uniformly distributed vacancies, therefore no localized deformation effect has been observed. A closer case to our study is the random distribution of unreconstructed defects in planar honeycomb lattices simulated by Whitty *et al* [40]. For re-entrant honeycombs (pristine Poisson's ratio -1.7), the deletion of vertical plus diagonal ribs for small volume fractions (<5%) leads to stiffness decreases of the order of 10%, and similar changes in terms of Poisson's ratio. However, there are some differences between the planar honeycomb lattice model in [40], and the SWCNT representation used in the present Monte Carlo analysis. In [40], the slenderness of the rib (16%) and the internal cell angle of the pristine unit cell make the flexural deflection of the rib itself as the main deformation mechanism of the whole honeycomb [50]. The C–C bond model used for these simulations imply very short beams (slenderness 60%), making therefore the shear deformation as the main deformation mechanism for the lattice structure [45], with significant changes to Poisson's ratios in uniform lattices [7]. Also in slender ribs assemblies, the introduction of small amounts of heterogeneity in regular honeycomb assemblies also leads to large fluctuations of Poisson's ratios, with $\Delta\nu = 1.70$ for pristine $\nu = 0.71$ [51]. The increased level of heterogeneity induced by the NRV defects in the SWCNT is therefore likely to augment the anisotropy of the lattice tube assemblies [49], amplified also by the coupling between axial and bending on the whole tube due to the localized deformations induced by the NRVs themselves.

The percentage of NPRs in the NRV tubes varies according to the nanotube chirality, aspect ratio and vacancy ratios. We have observed that the percentage of auxetic nanotubes varies between a 12.5% for an armchair (6, 6) at an aspect ratio of 5 and NRV of 0.5% to 33% for zigzag (27, 0), aspect ratio 20 and NRV of 2%. The percentage of auxetic nanotubes for a given radius appears to be linearly dependent on the tube aspect ratio and proportional to $\mathrm{NRV}^{1/2}$ for the vacancies. The mean values for the positive and negative PR values for a given tube aspect ratio appear also linearly dependent on the percentage of vacancies, as well as proportional to R^{-1}. In zigzag configurations (figure 5(*a*)), mean positive ν_{zr} varies between 12.7 for a radius of 0.297 nm and 2.31 for a chirality index n of 27, all for a NRV percentage of 2.0%. For the minimum vacancies ratio considered in this study, the positive mean Poisson's ratio is reported to be 1.04 for the same aspect ratio

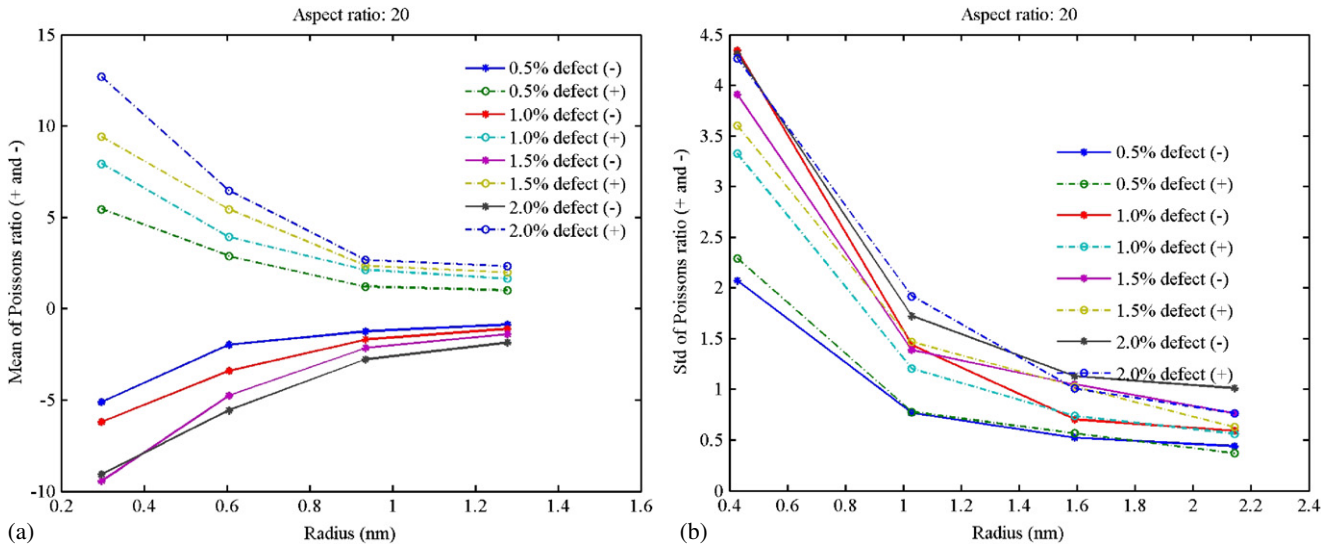

Figure 5. (*a*) Mean values for PPR and NPR for zigzag configurations and aspect ratio of 20 (pristine PR ranging between 0.22 and 0.16). (*b*) Distribution of the standard deviations for armchair configurations (pristine Poisson's ratios varying between 0.29 and 0.16).

and tube radius (AR = 20 and $R = 1.278$ nm, respectively). For the auxetic CNTs, the average Poisson's ratios range between −9.1 for $n = 6$ and NRV = 2.0% to −0.87 for $n = 27$ and NRV = 0.5%. The distribution of the standard deviations (figure 5(*b*)) again follows the inverse radius dependence and linear proportionality with the vacancies percentages, with a maximum of 7.9 for positive PR (6, 0) nanotubes at 2.0% of NRVs to a minimum of 0.58 for (27, 0) at 0.5%. The standard deviations for the auxetic nanotubes follow a similar trend, with a general decrease of 13–17% compared with the positive Poisson's ratio nanotubes. A similar behaviour has been also recorded for (n, n) nanotubes.

The mechanical behaviour of the NRD nanotubes could lead to some very interesting potential applications, such as nanoscillators, reinforcing fibres for nanocomposites and elastic strings in nanoscale energy storage devices. When assessing the advantages of auxetic (NPR) materials, it is seldom indicated that the negative Poisson's ratio could provide step changing improvements in the mechanical properties, when compared with PPR materials having the same stiffness. In reality, engineering solids obtained from transforming a PPR phase, such as open cell foams, tend to have a decrease in stiffness by a factor of 2–3 compared with their conventional counterpart [4, 52]. NRD nanotubes have only a slight decrease in stiffness (0.85–0.98), but could exhibit extreme values of Poisson's ratio. This feature can be very appealing as it could substantially enhance the structural stiffness of CNTs. Assuming an isotropic behaviour of the CNT, the bending stiffness of an elastic nano-shell can be estimated by $D_0 = Y_0 d^3/12/(1-\nu_0^2)$. Assuming a constant thickness d, the bending stiffness of the NRD nanotube would become $D \sim 0.9 Y_0 d^3/12/(1-\nu^2)$. Taking a pristine PR $\nu_0 \approx 0.16$ [43–48], the bending stiffness ratio between the NRD nanotube (armchair of zigzag) and pristine configuration would be $\sim 0.88/(1-\nu^2)$. Apart from Poisson's ratio interval $-0.34 < \nu_{rz} < 0.34$, the bending stiffness of a NRD nanotube would be significantly higher than the one of a pristine nanotube. In the extreme case when ν_{rz} approaches −0.99, the bending stiffness ratio would assume values close to 45. This suggests an increase in the fundamental frequency by a factor of 6.7 for NRD nanotubes as nano-resonators when modelled as Donnell–Vlasov thin shells [53]. Moreover, the critical buckling strain of CNTs under axial compression is proportional to their bending stiffness. Thus, the NRD nanotubes could achieve a critical value up to an order of magnitude greater than that of their pristine counterparts, even if the effect of the geometric imperfections due to vacancies is taken into consideration. However, the tensile strength and critical strain are significantly reduced compared with the pristine configuration [21, 38]. Accordingly, under axial compression, the strain energy density of CNT springs in energy storage devices would be raised considerably when the extreme value of Poisson's ratio is introduced in the presence of NRD vacancies.

Another noteworthy implication on having nanotubes with slightly reduced stiffness but large variations of Poisson's ratio compared with their pristine counterpart can also be found in the development of nanocomposites, especially based on the unidirectional ones. The use of variational methods (Hashin–Shritkman bounds (HS) [54]) to evaluate the overall bulk and shear modulus indicates that with auxetic isotropic inclusions having $\nu_{rz} \to -1$, the shear modulus of the composite calculated with the upper HS would tend towards infinity. In this case, the shear modulus ratio versus the composite configuration with pristine nanotubes would assume a value of 100 for $\nu_{rz} = -0.98$, a volume fraction of 7% and typical Young's modulus ratio Y/Y_m of 1000 between nanotubes and matrix. On the other hand, the bulk modulus of the nanocomposite would increase by 60% for similar volume fraction of isotropic inclusions with ν_{rz} approaching 0.49. In terms of unidirectional stiffness, a nanocomposite with NRD inclusions would have the 90% of Young's modulus of the pristine nanotube configuration. The structural integrity of the nanocomposites would also benefit by the presence of

this type of extreme Poisson's ratio nanotubes, especially for the fibre pullout characteristics. Let us assume we are using a typical epoxy-based matrix with a Poisson's ratio $\nu_m = 0.25$, and pristine CNTs inclusions of radius 1.27 nm and aspect ratio 20. If we consider a dry friction of 0.1 between the nanotubes and the matrix, the ratios between the linear maximum tensile membrane forces along the CNTs and maximum shear stresses for the defective and pristine configurations are, respectively [55]:

$$\frac{T}{T_0} = \frac{0.2724}{-1 + e^{-0.027\nu_{rz} - 0.3161}} \frac{\tau}{\tau_0} = \frac{0.0109\nu_{rz} + 0.2708}{1 - e^{-0.027\nu_{rz} - 0.3161}}. \quad (2)$$

While the maximum membrane force T would only change slightly compared with the pristine configuration (±5% from the most auxetic to positive PR values), the maximum shear stresses would be significantly reduced, from 67% with $\nu_{rz} = -0.98$ to 76% for $\nu_{rz} = 0.49$. The pullout of the nanofibres would also be impeded by the auxetic nanotube configurations, providing a lateral expansion against the surrounding matrix when subjected to tensile loading, as it occurs for auxetic polypropylene fibres [56] and NPR polyethylene yarns [57].

Acknowledgment

The authors acknowledge the partial support from the EU FP6 project STRP 01364 for the CPU time.

References

[1] Lakes R S 1993 *Adv. Mater.* **5** 293
[2] Love A E H 1944 *A Treatise on the Mathematical Theory of Elasticity* 4th edn (New York: Dover)
[3] Baughman R H, Shacklette J M, Zakhidov A A and Stafstrom S 1998 *Nature* **392** 362
[4] Lakes R S 1987 *Science* **235** 1038
[5] Herakovich C T 1984 *J. Compos. Mater.* **18** 447
[6] Alderson A and Evans K E 1997 *J. Mater. Sci.* **32** 2797
[7] Scarpa F, Panayiotou P and Tomlinson G 2000 *J. Strain Anal.* **35** 383
[8] Prall D and Lakes R 1996 *Int. J. Mech. Sci.* **39** 305
[9] Evans K E and Alderson A 2000 *Adv. Mater.* **12** 617
[10] Scarpa F, Blain S, Lew T, Perrott D, Ruzzene M and Yates J R 2007 *Compos A: Appl. Sci. Manuf.* **38** 280
[11] Lakes R S and Elms K 1993 *J. Compos. Mater.* **27** 1193
[12] Howell B, Prendergast P and Hansen L 1994 *Appl. Acoust.* **43** 141
[13] Scarpa F and Smith F C 2004 *J. Int. Mater. Struct.* **15** 973
[14] Shen L and Li J 2004 *Phys. Rev.* B **69** 045414
[15] Chang T and Gao H 2003 *J. Mech. Phys. Solids* **51** 1059
[16] Jindal P and Jindal V K 2006 *J. Comput. Theor. Nanosci.* **3** 148
[17] Yao Y T, Alderson A and Alderson K 2008 *Phys. Status Solidi* b **245** 2373
[18] Van Lier G, Van Alsenoy C, Van Doren V and Geerlings P 2000 *Chem. Phys. Lett.* **326** 181
[19] Yakobson B I and Couchman L S 2006 *J. Nanopart. Res.* **8** 105
[20] Lee J Hall, Coluci V R, Galvão D S, Kozlov M E, Zhang M, Dantas S O and Ray H Baughman 2008 *Science* **320** 504
[21] Sammalkorpi M, Krasheninnikov A, Kuronen A, Nordlund K and Kaski K 2004 *Phys. Rev.* B **70** 245416
[22] Gao R P, Wang Z L, Bai Z G, de heer W A, Dai L M and Gao M 2000 *Phys. Rev. Lett.* **85** 622
[23] Mawhinney D B, Naumenko V, Kuznetsova A, Yates J T Jr, Liu J and Smalley R E 2000 *Chem. Phys. Lett.* **324** 213
[24] Andrews R, Jacques D, Qian D and Dickey E C 2001 *Carbon* **39** 1681
[25] Ni B, Andrews R, Jacques D, Qian D, Wijesundara M B J, Choi Y, Hanley L and Sinnott S B 2001 *Appl. Phys. A: Mater. Sci. Process.* **105** 12719
[26] Ni B and Sinnott S B 2000 *Phys. Rev.* B **61** R16343
[27] Terrones M, Banhart F, Grobert N, Charlier J C, Terrones H and Ajayan P 2002 *Phys. Rev. Lett.* **89** 075505
[28] Hu Y, Jang I and Sinnott S B 2003 *Compos. Sci. Technol.* **63** 1663
[29] Krasheninnikov A V 2001 *Solid State Commun.* **118** 361–5
[30] Wang C and Wang C Y 2006 *Eur. Phys. J.* B **54** 243–47
[31] Zhou L G and San-Qiang Shi 2003 *Appl. Phys. Lett.* **83** 1222–4
[32] Miyamoto Y, Rubio A, Berber S, Yoon M and Tománek D 2004 *Phys. Rev.* B **69** 121413
[33] Vandescuren M, Amara H, Langlet R and Lambin P 2007 *Carbon* **45** 349–56
[34] Dinadayalane T C and Leszczynski J 2007 *Chem. Phys. Lett.* **434** 86–91
[35] Ajayan P M, Ravikumar V and Charlier J C 1998 *Phys. Rev. Lett.* **81** 1437
[36] Krasheninnikov A V, Nordlund K, Sirviö M, Salonen E and Keinonen J 2001 *Phys. Rev.* B **63** 245405
[37] Krasheninnikov A V and Banhart F 2007 *Nature Mater.* **6** 723
[38] Hou W and Xiao S 2007 *J. Nanosci. Nanotechnol.* **7** 4478
[39] Smith C W, Grima J and Evans K E 2000 *Acta Mater.* **48** 4349
[40] Whitty J P M, Alderson A, Myler P and Kandola B 2003 *Composites* A **34** 525
[41] Li C and Chou T W 2003 *Int. J. Solids Struct.* **40** 2487
[42] Li C and Chou T W 2003 *Compos. Sci. Technol.* **63** 1517
[43] Shenderova O A, Zhirnov V V and Brenner D W 2002 *Crit. Rev. Solid State Mater. Sci.* **27** 227
[44] Scarpa F and Adhikari S 2008 *J. Phys. D: App. Phys.* **41** 085306
[45] Scarpa F, Adhikari S and Srikantha Phani A 2009 *Nanotechnology* **20** 065709
[46] ANSYS Inc. *ANSYS Multiphysics*, Canonsburg, PA, USA http://www.ansys.com
[47] Timoshenko S P and Goodier J N 1970 *Theory of Elasticity* 3rd edn (New York: McGraw-Hill)
[48] Wang L F, Zheng Q S, Liu J and Jiang Q 2005 *Phys. Rev. Lett.* **95** 105501
[49] Scarpa F, Smith C W, Ruzzene M and Wadee M K 2008 *Phys. Status Solidi* b **245** 584
[50] Gibson L J and Ashby M F 1997 *Cellular Structures—Structure and Properties* 2nd edn (Cambridge: Cambridge University Press)
[51] Horrigan E J, Smith C W, Scarpa F L, Gaspar N, Javadi A A, Berger M A and Evans K E 2009 *Mech. Mater.* **41** 919
[52] Bianchi M, Scarpa F and Smith C W 2008 *J. Mater. Sci.* **43** 5851
[53] Lu P, Lee H P, Lu C and Chen H B 2008 *Int. J. Mech. Sci.* **50** 501
[54] Hashin Z and Shtrikman S 1963 *J. Mech. Phys. Solids* **11** 127
[55] Xiao T and Liao K 2004 *Composites* B **35** 211
[56] Simkins V R, Alderson A, Davies P J and Alderson K L 2005 *J. Mater. Sci.* **40** 4355
[57] Miller W, Hook P B, Smith C W, Wang X and Evans K E 2009 *Compos. Sci. Technol.* **69** 651